Comparison of Control Techniques Applied to Photovoltaic Boost Converters

Henrique Horst Figueira, Lucas Vizzotto Bellinaso, Leandro Michels
Grupo de Eletrônica de Potência e Controle - GEPOC
Universidade Federal de Santa Maria - UFSM
henrique.labensaios@gepoc.ufsm.br, lucas@gepoc.ufsm.br, michels@gepoc.ufsm.br

Mauro Fernando Basquera Jr.
PHB Eletrônica Ltda.
São Paulo – SP, Brazil
mauro@phb.com.br

***Abstract* — Grid-tie photovoltaic (PV) inverters are usually composed of two conversion stages: a dc-dc boost converter and a dc-ac converter. The dc-dc boost converter is mainly responsible for extracting the maximum power from the photovoltaic array. Several control strategies have been proposed in the literature for controlling the dc-dc boost converter. However, PV systems have characteristics that impact on transient and steady state response because its small signal model is irradiance-dependent and its dc bus has oscillations (120Hz) due to inverter modulation. Thus in order to contribute to this field and support control designers, this manuscript compares three control strategies applied to PV boost converters: a simple perturbation and observation (P&O) maximum power point tracking (MPPT) algorithm controlling directly the duty cycle; a MPPT algorithm associated with a voltage controller; and a MPPT algorithm with cascaded voltage and current control. Experimental results are presented for comparison. Results show the third strategy (MPPT with cascade control) provides the best results for most comparison criteria.**

Keywords— Photovoltaic power systems, boost converter, digital control, Maximum Power Point Tracking.

I. INTRODUCTION

Grid-tie photovoltaic (PV) inverters are usually composed of two power conversion stages in low power applications (up to 6 kW). The first stage is one or more dc-dc converters that step-up the PV array voltage as well as track the Maximum Power Point (MPP). The second stage is a dc-ac converter designed to inject power into grid [1]. Fig. 1 shows a two-stage system for a single-phase inverter.

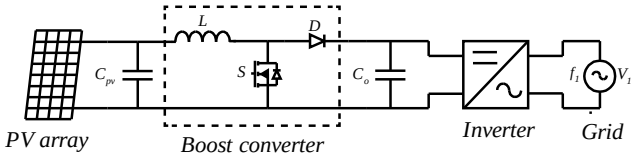

Fig. 1. Grid-tie PV system with boost converter.

Due to its simplicity, the most employed converter topology in the first stage is the conventional dc-dc boost converter. However, for this application, there are several important requirements that have to be considered:

i) high efficiency of Maximum Power Point Tracking (MPPT) of the PV system [2]–[4];

ii) operation in both continuous conduction mode (CCM) and discontinuous conduction mode (DCM) with fast transient response [5], [6];

iii) when PV power extraction must be limited, such as due to operational restrictions defined by PV inverter standards, the converter control must change from MPPT mode to Limited Power Tracking (LPT) mode [7], performing a precise control of inductor current;

iv) long life-time, which can be achieved by using film capacitors instead of electrolytic capacitor at the PV array output and dc-link (C_{pv}).

Many MPPT techniques control directly the duty cycle of the boost converter [8]-[10], but cannot control the inductor current. Other MPPT techniques provide current or voltage reference to the control system of the boost converter [11]. The current reference is strongly dependent on the solar irradiance, while the voltage remains approximately constant when the irradiance changes [12]. For this reason, MPPT algorithms whose output is the PV voltage reference are usually more appropriate.

In a cascade control system, the MPPT algorithm generates the PV voltage reference, a voltage control generates the inductor current reference, and an internal current loop generates the duty cycle of the converter [13]. With this control scheme, the steady-state requirements (i), (ii) and (iv) can be easily achieved. However, when low capacitance film capacitors are used, the small-signal equivalent resistance of the PV system directly affects the control dynamic response, which becomes dependent on the irradiance and the I-V curve operation point.

The most usual solution to mitigate this problem is to employ a capacitor (C_{pv}) with a capacitance greater than the required. In this case, the poles of the current and voltage models are moved to lower frequencies, which allows simplifying both models to simple integrators. However, this alternative reduces the speed of dynamic response of the voltage loop. In addition, it may require electrolytic capacitors, which usually implies a reduction in system life and increase losses. This dependence is a problem when the converter must attend all requirements from (i) to (iv).

Urtasun et al. [14] proposed an adaptive voltage controller to overcome these problems based on the estimation of the equivalent resistance of the photovoltaic system, measured at the inverter disturbance frequency (100/120 Hz). However, this strategy is dependent on the ripple generated by inverter, limiting its dynamic response speed. Additionally, no results were presented considering

the converter in discontinuous conduction mode. Bianconi et al [15] presented a sliding-mode voltage controller, however the proposed technique requires an extra current sensor, which increases the cost of the application.

This manuscript compares three different control strategies applied to the PV boost stage. The control strategies evaluated are i) Perturb and Observe (P&O) MPPT; ii) P&O MPPT with voltage control and iii) P&O with cascaded voltage and current control. The following aspects are evaluated: i) current settling time for an irradiation step; ii) disturbance rejection in the input capacitor; iii) average output power extracted. First, the PV array model and the controllers are described in Section II. Then, Section III covers the controllers design. Experimental results, comparison and discussion are shown in Section IV, followed by conclusion.

II. SYSTEM DESCRIPTION

A PV system with dc-dc boost converter and a single-phase inverter can be represented by the equivalent circuit of Fig. 2 at any operation point. The Norton equivalent current source is proportional to the irradiance (G), while the equivalent resistance (r_{pv}) is the derivative of the PV voltage by current at the I-V curve operation point.

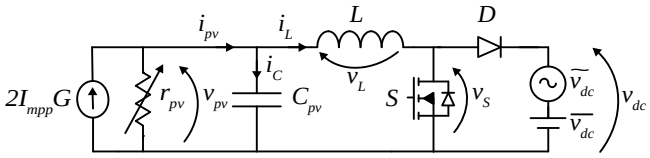

Fig. 2. Equivalent model of two stage PV system.

At the Maximum Power Point (MPP), the equivalent resistance r_{pv} is dependent on the irradiance and temperature. Fig. 3 shows r_{pv} at the MPP for a PV array composed by polycrystalline silicon modules. The parameters of the PV array are shown in Table I. One can observe that r_{pv} at 50 W/m² is around 5 times higher than at 1000 W/m². In addition, the resistance is more dependent on the temperature at low irradiances.

TABLE I. PARAMETERS OF PV ARRAY AT 1000 W/M² AND 25°C

Parameter	Value
PV maximum power point voltage (V_{mpp})	70.8 V
PV open-circuit voltage (V_{oc})	87.6 V
PV maximum power point current (I_{mpp})	7.38 A
PV short-circuit current (I_{sc})	7.65 A

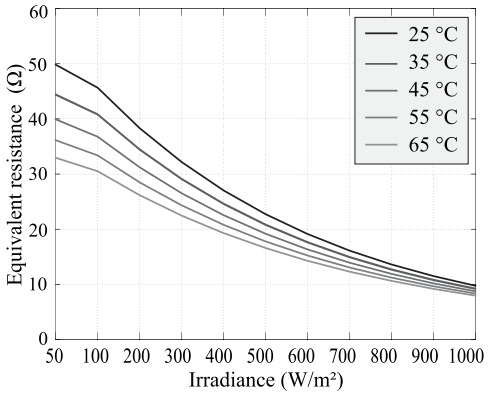

Fig. 3. PV equivalent resistance around MPP for different irradiance levels under different temperatures.

A. Strategy 1 –MPPT controlling duty cycle

The first control strategy evaluated is the Perturb and Observe (P&O) directly generating dc-dc converter duty cycle. This method of tracking the Maximum Power Point Tracking (MPPT) does not require a previous knowledge of the employed PV array. As shown in Fig. 4(a), this MPPT technique requires PV voltage and current measurement to calculate PV power. The duty cycle (d_s) is changed with fixed steps at a constant frequency. The step signal (+ | –) is chosen as the one which increased power in the last sample period. This process leads the PV system towards the MPP [10].

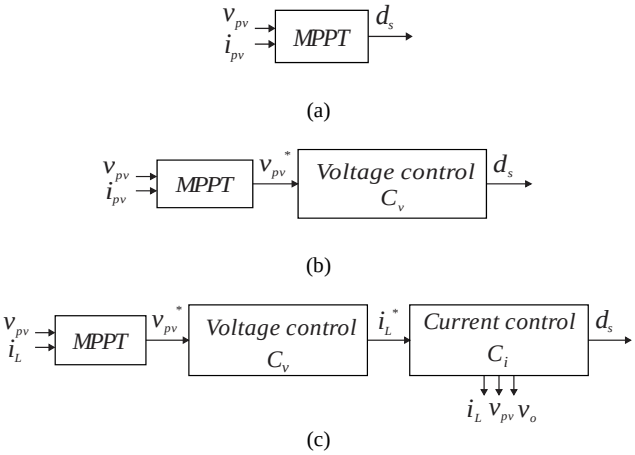

Fig. 4. Control diagram: (a) MPPT controllind duty cycle, (b) MPPT and voltage control and (c) MPPT and cascade voltage and current control.

B. Strategy 2 – MPPT and voltage control

The second control strategy evaluated includes a linear voltage controller which controls duty cycle (d_s). As shown in the block diagram of Fig. 4(b), there is still an MPPT algorithm (P&O), which controls voltage reference (v_{pv}^*) instead of d_s. The transfer function that relates v_{pv} and the complementary duty cycle $d_{s1} = (1 - d_s)$ is given by (1). This transfer function is used to design the controller, which generates d_{s1} and then duty cycle is calculated by $d_s = 1 - d_{s1}$.

$$G_{V_1}(s)=\frac{V_{pv}(s)}{(1-D_s)(s)}=v_o\left(\frac{\frac{1}{C_{pv}L}}{s^2+\frac{1}{C_{pv}r_{pv}(G)}s+\frac{1}{C_{pv}L}}\right) \quad (1)$$

C. Strategy 3 – MPPT and cascaded voltage and current control

The third control strategy evaluated is composed by an P&O MPPT algorithm which generates PV voltage reference, and a cascade linear voltage and current control, where the voltage controller generates the reference to the inner current loop. This approach was proposed in [16] and [17] and allows a decoupling between the dc-ac converter disturbance and the v_{pv}. Figure 4(c) presents the block diagram of this control strategy. A non-linear current controller has been chosen because a usual linear controller may interact with the voltage controller when the PV capacitance is too small [16]. Besides that, this non-linear controller does not interact with the voltage controller, and is robust to variation of the PV array equivalent resistance r_{pv}.

The transfer function that relates V_{pv} and the boost inductor current (I_L) is given by (2).

$$G_v(s)=\frac{V_{pv}(s)}{I_L(s)}=-\frac{r_{pv}(G)}{C_{pv}r_{pv}(G)s+1} \quad (2)$$

The transfer function that relates the boost inductor current (I_L) and the boost duty cycle (d_s) is given by (3)

$$\frac{I_L(s)}{D_s(s)}=-\frac{v_o\left(C_{pv}r_{pv}(G)+1\right)}{r_{pv}(G)}\left(\frac{\frac{1}{LC_{pv}}}{s^2+\frac{1}{C_{pv}r_{pv}(G)}s+\frac{1}{LC_{pv}}}\right) \quad (3)$$

III. CONTROL DESING

Three control schemes have been implemented. The boost converter parameters are show in Table II.

TABLE II. BOOST CONVERTER PARAMETERS

Parameter	Value
Input voltage (V_{pv})	70.80 V
Output voltage (V_o)	220.00 V
Inductor current ripple (Δ_{IL})	30% Isc
Boost inductor (L)	530 µH
PV output capacitor (C_{pv})	3.30 µF
Switching frequency (f_s)	40 kHz
Duty cycle for MPP (D_{mpp})	0.678

A. Strategy 1 – MPPT controlling duty cycle

The Perturb & Observe MPPT was designed as [18]. The defined sampling period for was 25 µs and the duty cycle step for perturbation was 0.005.

B. Strategy 2 – MPPT and voltage control

Table III shows the requirements used for designing the voltage control.

TABLE III. VOLTAGE CONTROL REQUIREMENTS

Parameter	Value
Cut-off frequency	< 1 kHz
Gain margin (GM)	> 6 dB
Phase margin (PM)	> 60º
Settling time	< 10 ms
Zero voltage overshoot High gain at 120 Hz Zero steady state error	

To achieve these specifications a Proportional Integral (PI) compensator was design using Matlab. The zero is placed at high frequency to optimize the dynamic response [19-20]. The designed controller transfer function is:

$$C_{v_1}(z)=0.00039155\frac{(z-0{,}158)}{(z-1)} \quad (4)$$

A cut-off frequency of 468 Hz, GM of 7 dB, PM of 83.6º and 12 dB open-loop gain at 120 Hz were obtained. The settling time depends on the irradiance, resulting 1.25 ms and 1.06 ms for 50 W/m² and 1000 W/m² respectively.

C. Strategy 3 – MPPT and cascaded voltage and current control

1) Current control

The non-linear current control structure is presented in Fig. 5 [19]. The transfer function C_i consists of a conventional linear controller and provides the inductor voltage reference (v_L^*). The voltage reference v_L^* is related through the Kirchhoff's voltage law using switch voltage (v_s) and PV array voltage (v_{pv}). This scheme allows the controller to attenuate 120 Hz disturbances.

Eq. (5) and Eq. (6) provide the control action that allows the operation in the Continuous Condition Mode (CCM) and Discontinuous Condition Mode (DCM), respectively. The subsequent block selects the duty cycle to be applied to the boost converter.

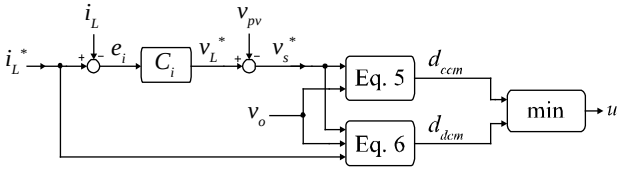

Fig. 5. Block diagram of proposed non-linear current control.

$$d_{ccm}=1-\frac{v_s^*}{v_o} \quad (5)$$

$$d_{dcm}=\sqrt{\frac{2Li_L^*\left(v_o-v_s^*\right)}{T_s v_o v_s^*}} \quad (6)$$

The transfer function that relates the inductor boost current (I_L) and its average voltage is given by:

$$G_i(s)=\frac{I_L(s)}{\langle V_L(s)\rangle}=\frac{1}{sL} \quad (7)$$

The linear controller which calculates v_L^* was designed considering the specification given in Table IV.

TABLE IV. CURRENT CONTROL REQUIREMENTS

Parameter	Value
Cut-off frequency	2.5 kHz < f_{Gi} < 4 kHz
Gain margin (GM)	> 6 dB
Phase margin (PM)	> 50º
Settling time	< 1 ms
Current over shoot < 20% High gain at 120 Hz Zero steady state error	

A lead-lag resonant controller was designed:

$$C_i(z) = 8.1 + \frac{z-0.795}{z-0.164} + ... + \frac{z^2 - 1.984353560585123z + 0.984414763351714}{z^2 - 1.999644327837542z + 1} \quad (8)$$

It was achieved a cut-off frequency of 2.63 kHz, GM of 10 dB, PM of 50.5º and 150 dB gain at 120 Hz. The settling time was 0.4 ms with overshoot lower than 20%.

2) Voltage control

Table V shows the requirements considered to design the linear voltage control. It is important to highlight that the transfer function G_v depends on r_{pv}. Thus, the controller was designed for the lower irradiance case of 50W/m² due to its higher cut-off frequency.

TABLE V. VOLTAGE CONTROL REQUIREMENTS

Parameter	Value
Cut-off frequency	< 0.1 f_{Gi}
Gain margin (GM)	> 6 dB
Phase margin (PM)	> 60º
Settling time	< 1 s
Zero Voltage over shoot Zero steady state error	

To meet these requirements, the following PI controller was designed:

$$C_{v2}(z) = -0.01385\frac{(z-0.483)}{(z-1)} \quad (9)$$

Considering 50 W/m² irradiance, it was achieved a cut-off frequency of 203 Hz, GM of 11 dB, PM of 92º, and a settling time of 2.85 ms. For 1000 W/m², the cut-off frequency was 44 Hz, GM of 20 dB, PM of 91.7º and a settling time response of 14.82 ms.

IV. EXPERIMENTAL RESULTS AND DISCUSSION

Experimental results have been obtained to compare the control schemes. Three comparison criteria have been chosen for comparison: settling time, 120 Hz disturbance rejection, and maximum power extracted. All comparisons have been carried out for the same test conditions.

The experimental setup is shown in Fig. 6. The controllers were implemented using the DSP TMS320F28335 (Texas Instruments). The dc-ac bus was emulated with an ac power source configured with a dc offset of 220 V added to a 120 Hz oscillation with 5 V amplitude.

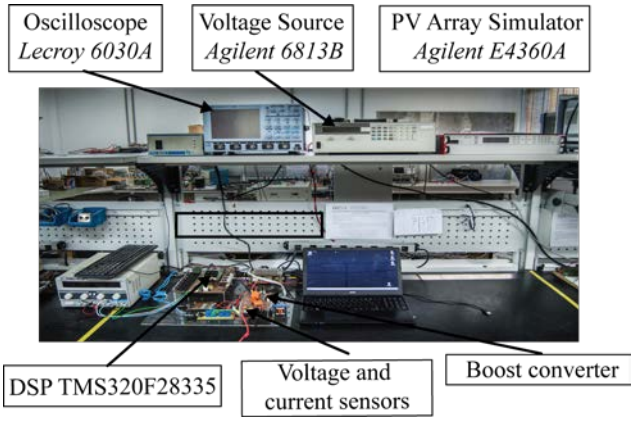

Fig. 6. Experimental setup.

1) Settling time

Two tests were performed considering abrupt irradiance variations. Fig. 7 (a), (b) and (c) show the response for a step from 0 W/m² to 50 W/m², which is when the boost converter is operating under DCM. The first strategy was not able to find the MPP in this case. The settling time for strategies 2 and 3 were about 8 ms. Fig. 8 (a), (b) and (c) show a step from 0 W/m² to 1000 W/m². All strategies could track the MPP, and the settling time for strategies 1, 2 and 3 are 1.47 ms, 1.48 ms and 23.73 ms, respectively. The higher settling time of strategy 3 is due to the decrease of the plant's gain when the irradiance increases.

2) Disturbance rejection

This test was performed at standard test conditions (1000 W/m²). Fig. 9 (a), (b) and (c) present the voltage disturbance for strategies 1, 2 and 3. Strategy 1 was not able to reject any disturbance and presents the worst performance. Strategy 2 attenuates 120 Hz oscillation. Finally, strategy 3 has the best performance, rejecting all 120 Hz oscillations due to its resonant controller.

3) Maximum power extracted

This test was performed at standard test conditions (1000 W/m²). Fig. 10 (a), (b) and (c) show the extracted power for strategies 1, 2 and 3. The extracted powers were 521.13 W, 540.02 W and 542.43 W, respectively. It is important to highlight that, as the irradiance reduces, and the boost enters in DCM, the MPPT from strategy 1 loses performance, as demonstrated in Fig. 7(a). Comparing strategies 2 and 3, strategy 3 extracts an extra 2.32 W due to 120 Hz rejection.

Table VI summarizes the comparative analysis presented in this manuscript. Strategy 1 had the worst results for all criteria's. Strategy 2 has lower settling time lower comparing to strategy 3 at high irradiance, but does completely not rejects 120 Hz oscillations, reducing the maximum extracted power. Finally, only the strategy 3 can limit the extracted power by controlling the inner current loop reference. Therefore, it can be seen that strategy 3 (MPPT and cascaded voltage and current control) is the best strategy for most applications, effectively reducing 120 Hz oscillations and enabling power limitation.

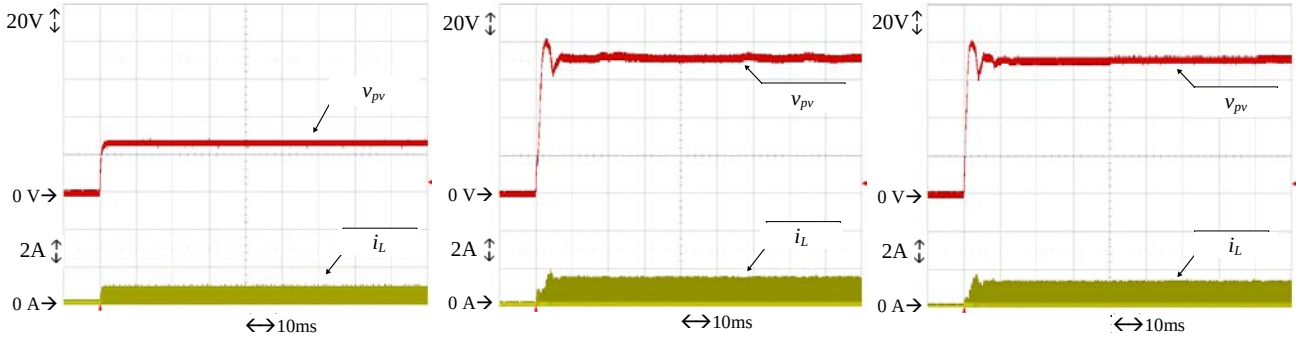

Fig. 7. Irradiance step from 0 to 50 W/m²: (a) MPPT controlling duty cycle; (b) MPPT and voltage control; (c) MPPT and cascade V and I control.

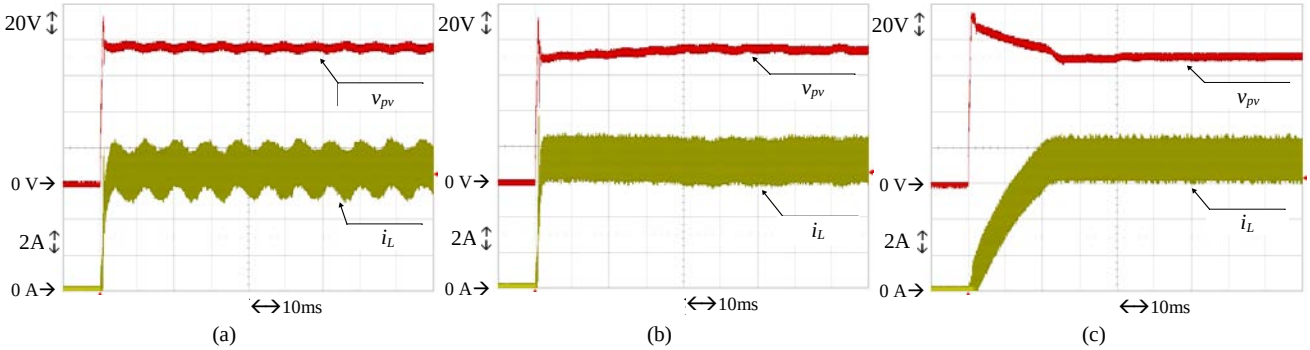

Fig. 8. Irradiance step from 0 to 1000 W/m²: (a) MPPT controlling duty cycle; (b) MPPT and voltage control; (c) MPPT and cascade V and I control.

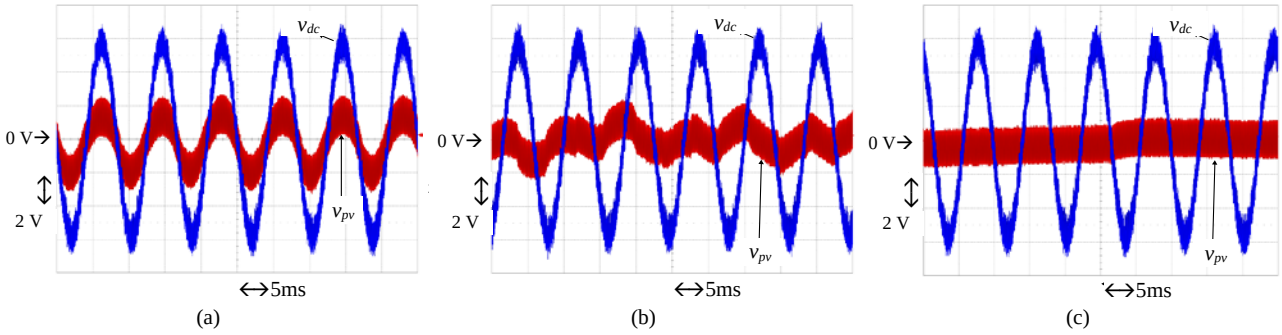

Fig. 9. Disturbance rejection: (a) MPPT controlling duty cycle; (b) MPPT and voltage control; (c) MPPT and cascade V and I control.

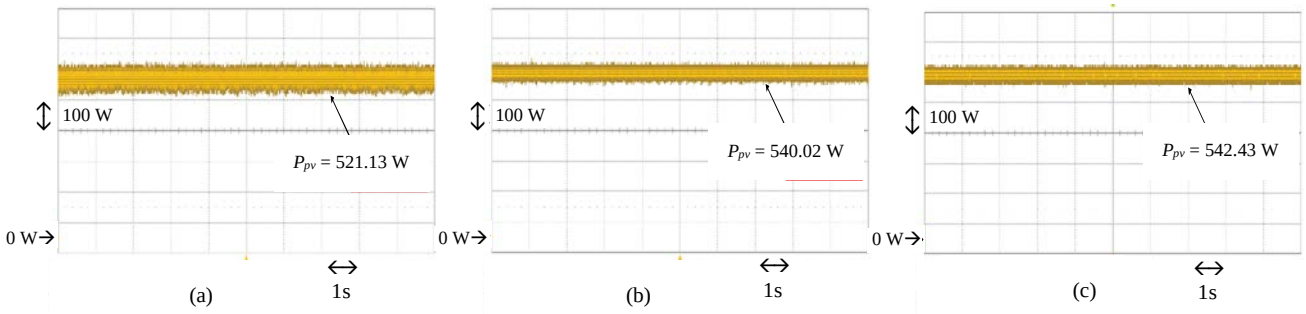

Fig. 10. Maximum power extracted: (a) MPPT controlling duty cycle; (b) MPPT and voltage control; (c) MPPT and cascade V and I control.

TABLE VI. STRATEGIES COMPARISON

Parameter	Strategy 1 MPPT	Strategy 2 MPPT & voltage control	Strategy 3 MPPT & cascade control
Dynamic response	- (50 W/m²) 1.479 ms (1000 W/m²)	8.478 ms (50 W/m²) 1.484 ms (1000 W/m²)	8.857 ms (50 W/m²) 23.73 ms (1000 W/m²)
Disturbance rejection	none	poor	good
Power extracted	521.13 W	540.02 W	542.43 W

V. CONCLUSION

This manuscript presented a comparison of three different control strategies applied to the dc-dc stage of grid-tie PV inverter. The first strategy was a P&O MPPT, the second strategy was a P&O MPPT with a linear voltage control. The last strategy was a P&O MPPT with a cascade linear voltage and non-linear current control. The adopted comparison criteria were settling time, 120 Hz disturbance rejection and maximum power extracted. Experimental results showed the first strategy had the worst performance for all three criteria. The second strategy had a good dynamic response and power extraction but could not effectively reject 120 Hz disturbances. Finally, the third strategy had the best overall performance and, in addition, this strategy could operate out of the MPP, which is a standard requirement for grid-tie inverters.

ACKNOLEDGEMENTS

The authors thank INCTGD, CAPES, CNPq and FAPERGS for the financial support received for the development of this work. L. Michels were supported by a research grant of CNPq—Brasil. This work was carried out with the support of INCT and its funding agencies (CNPq process 465640 / 2014-1, CAPES process No. 23038.000776 / 2017-54 and FAPERGS 17 / 2551-0000517-1) and CAPES-PROEX.

REFERENCES

[1] S. B. Kjaer, J. K. Pedersen, and F. Blaabjerg, “A Review of Single-Phase Grid-Connected Inverters for Photovoltaic Modules,” in *IEEE Trans. Ind. Appl.*, 2005, vol. 41, no. 5, pp. 1292–1306.

[2] T. Esram and P. L. Chapman, “Comparison of Photovoltaic Array Maximum Power Point Tracking Techniques,” in *IEEE Trans. Energy Convers.*, 2007, pp. 439–449.

[3] S. B. Kjaer, J. K. Pedersen, and F. Blaabjerg, “A Review of Single-Phase Grid-Connected Inverters for Photovoltaic Modules,” in *IEEE Trans. Ind. Appl.*, 2005, pp. 1292–1306.

[4] P. de Assis Sobreira, M. G. Villalva, P. G. Barbosa, H. A. C. Braga, J. R. Gazoli, E. Ruppert, and A. A. Ferreira, “Comparative analysis of current and voltage-controlled photovoltaic Maximum Power Point tracking,” in *XI Brazilian Power Electronics Conference*, 2011, pp. 858–863.

[5] S. A. Papathanassiou, P. S. Georgilakis, and E. I. Batzelis, “Energy models for photovoltaic systems under partial shading conditions: a comprehensive review,” in *IET Renew. Power Gener.*, 2015, pp. 340–349.

[6] [6] S. Lyden, M. E. Haque, A. Gargoom, and M. Negnevitsky, “Review of Maximum Power Point Tracking approaches suitable for PV systems under Partial Shading Conditions,” in *2013 Australasian Universities Power Engineering Conference (AUPEC)*, 2013, pp. 1–6.

[7] [7] A. Urtasun, P. Sanchis, and L. Marroyo, “Limiting the power generated by a photovoltaic system,” in *10th International Multi-Conferences on Systems, Signals & Devices 2013 (SSD13)*, 2013, pp. 1–6.

[8] J. Tanouti, M. Setti, A. Aziz, and E. M. Aziz, “Application of feedback-feedforward loop digital control to a PWM dc-dc boost converter used for solar photovoltaic systems,” in *2014 International Renewable and Sustainable Energy Conference (IRSEC)*, 2014, pp. 747–752.

[9] R. Kotti and W. Shireen, “An efficient robust MPPT control for grid-connected photovoltaic systems with reduced DC link capacitance,” in *IECON 2014 - 40th Annual Conference of the IEEE Industrial Electronics Society*, 2014, pp. 5462–5467.

[10] N. Femia, G. Petrone, G. Spagnuolo and M. Vitelli, "A technique for improving P&O MPPT performances of double-stage grid-connected photovoltaic systems," in *IEEE Transactions on Industrial Electronics*, 2009, vol. 56, no. 11, pp. 4473-4482,

[11] P. E. Kakosimos, A. G. Kladas, and S. N. Manias, “Fast Photovoltaic-System Voltage- or Current-Oriented MPPT Employing a Predictive Digital Current-Controlled Converter” in *IEEE Trans. Ind. Electron.*, 2013. vol. 60, no. 12, pp. 5673–5685,

[12] D. Sera, R. Teodorescu, and P. Rodriguez, “PV panel model based on datasheet values,” in *2007 IEEE International Symposium on Industrial Electronics*, 2007, pp. 2392–2396.

[13] J. L. Agorreta, L. Reinaldos, R. Gonzalez, M. Borrega, J. Balda, and L. Marroyo, “Fuzzy Switching Technique Applied to PWM Boost Converter Operating in Mixed Conduction Mode for PV Systems,” *IEEE Trans. Ind. Electron.*, 2009, vol. 56, no. 11, pp. 4363–4373.

[14] A. Urtasun, P. Sanchis, and L. Marroyo, “Adaptive Voltage Control of the DC/DC Boost Stage in PV Converters With Small Input Capacitor,” in *IEEE Trans. Power Electron.*, 2013, vol. 28, no. 11, pp. 5038–5048.

[15] E. Bianconi, J. Calvente, R. Giral, E. Mamarelis, G. Petrone, C. A. Ramos-Paja, G. Spagnuolo, and M. Vitelli, “A Fast Current-Based MPPT Technique Employing Sliding Mode Control,” in *IEEE Trans. Ind. Electron.*, 2013, pp. 1168–1178,.

[16] L. V. Bellinaso, R. P. Vieira, H. A. Grundling, and L. Michels, “Adaptive control of PV boost converter for minimal passive components and fast maximum power point tracking,” in *2014 11th IEEE/IAS International Conference on Industry Applications*, 2014, vol. 4, pp. 1–7.

[17] L. V. Bellinaso, M. F. Basquera, R. P. Vieira, H. A. Grundling, and L. Michels, “Cascaded MPPT control with adaptive voltage controller applied to boost converters for PV applications,” in *2017 Brazilian Power Electronics Conference (COBEP)*, 2017, pp. 1–6.

[18] S. Pukhrem, “Comparative analysis of photovoltaic maximum power point tracking (MPPT) algorithm,” in *Power and Energy Student Summit (PESS)*, 2015, pp. 72–77.

[19] L. Roggia, J. E. Baggio, L. Michels, and J. R. Pinheiro, “Controladores para conversor Boost PFC operando nos Modos de Condução Contínua e Descontínua,” in *16th Autom. Brazil. Conf.*, 2008.